Supporting Information

Stress-dissipative strong bimodal molecular packing towards efficient and highly stretchable organic photovoltaics

Jiayuan Zhu,[a] Hongxiang Li,[a] Heng Wang,[a] Yufei Gong,[b] Yonghuan Li,[e] Yetai Cheng,[e] Yiling Hu,[a] Jie Xiong,[a] Jiayu Wang,[a] Lei Meng,[b] Jin Fang,[c] Wenjun Zou,[c,d] Yifan Wang,[e] Yuqiang Liu,[e] Cenqi Yan,*[a] Yongfang Li,[b] Pei Cheng*[a]*

[a]College of Polymer Science and Engineering, National Key Laboratory of Advanced Polymer Materials, Sichuan University, Chengdu 610065, China

[b]Beijing National Laboratory for Molecular Sciences, CAS Key Laboratory of Organic Solids, Institute of Chemistry, Chinese Academy of Sciences, Beijing 100190, China

[c]Hyper PV Technology Co., Ltd, Jiaxing 314000, China

[d]National Center for Nanoscience and Technology, Beijing 100190, China

[e]College of Textiles & Clothing, State Key Laboratory of Bio-fibers and Eco-textiles, College of Materials Science and Engineering, Qingdao University, Qingdao 266071, China

E-mail: lihongxiang@scu.edu.cn, yancenqi@scu.edu.cn, chengpei@scu.edu.cn

Materials

2PACz was purchased from Hyper PV Technology Co., Ltd. PM6, PBQx-TCl, PTQ10, BTP-eC9, PY-IT and PDINN were purchased from Solarmer Materials Inc. and were used without any further purification. PTB7-Th was purchased from 1-material. 1-Chlorohexadecane was purchased from J&K Scientific, Inc. Silver was purchased from ZhongNuo Advanced Material (Beijing) Technology Co., Ltd. The other materials and solvents were common commercial level and used as received. The Mn of PM6 we used was 39.5 kg/mol, with a dispersity of 1.93.

Device and Film Fabrication

OPV devices were fabricated in device configuration of ITO/2PACz/active layers/PDINN/Ag. The ITO substrates were first scrubbed by detergent and then sonicated with deionized water, acetone and isopropanol subsequently, and dried overnight in an oven. The glass substrates were treated by UV-Ozone for 20 min before use. 2PACz was spin cast onto the ITO substrates at 3000 rpm for 30 s, and then dried at 100 °C for 5 min in a nitrogen-filled glove box. For the OPVs without 1-Chlorohexadecane (Cl-16C), the polymer donor PM6 was dissolved in chloroform to prepare the donor solution with a concentration of 10 mg/ml and the solution was stirred for 1h on a hotplate at 50°C in a nitrogen-filled glove box. PM6 solution was spin-cast at 2400 rpm for 40 s. For the OPVs with Cl-16C, the polymer donor PM6 was dissolved in chloroform to prepare the donor solution with a concentration of 9 mg/ml and the 10 vol% Cl-16C was added as an additive and the solution was stirred for 1h on a hotplate at 50°C in a nitrogen-filled glove box. PM6 with Cl-16C solution was spin-cast at 2800 rpm for 40 s. Then, the device was heat-treated for 5 min at 100 °C. The molecule acceptor BTP-eC9 was dissolved in chloroform to prepare the acceptor solution with a concentration of 8 mg/ml and the 0.25 vol% DIO was added as an additive. The solution was stirred for 1h on a hotplate at 50°C in a nitrogen-filled glove box. BTP-eC9 solution was spin-cast at 3000 rpm for 40 s. Then, the device was heat-treated for 5 min at 100 °C. PDINN was dissolved in methanol to produce a solution with a concentration of 1 mg/mL. The PDINN solution was coated on the active layer at speed of 3000 rpm for 30 s. Eventually, a 100 nm Ag layer was deposited onto the surface via thermal evaporation. The thin film preparation process used for tensile testing and characterization was the same as the preparation of the active layer of the device.

The protocol for preparing strained samples for GIWAXS analysis

OTS-Modified Substrates: Cleaned silicon wafers (1.5×1.5 cm^2) were sequentially ultrasonicated in deionized water and isopropanol (10 min each), treated with UV-ozone for 20 min, coated with an OTS trichloroethylene solution (10 sec self-assembly followed by spin-coating at 3000 rpm for 30 sec), cured in an ammonia atmosphere for 10 hours, and finally ultrasonicated in toluene and deionized water.

SEBS-Modified Substrates: Cleaned silicon wafers (1.5×1.5 cm^2) were sequentially ultrasonicated in deionized water and isopropanol (10 min each). A SEBS solution in toluene was then spin-coated onto the substrates at 3000 rpm for 1 minute.

Preparation for the strained GIWAXS samples: The donor solution was spin-coated onto OTS-modified substrates under the same conditions used for OPV device fabrication. The resulting film was transferred from the OTS substrate onto a PDMS strip. The PDMS strip was stretched to apply the desired tensile strain to the film. The strained film was then transferred onto a SEBS-modified substrate for GIWAXS measurement.

Instruments and Characterizations

The *J*-*V* curves were measured under a computer-controlled Keysight B2900 source meter under 100 mW cm^{-2}, AM 1.5 G solar simulator (Enlitech SS-X50). The *J*-*V* curves were measured with forward scan mode from -0.2 V to 1 V, and the scan step was 0.01 V with a dwell time of 0.01 s. The light intensity was calibrated by a standard silicon solar cell to give a range from 0.99 to 1.01 sun. The EQE spectra were received from a commercial QE measurement system (Taiwan, Enlitech, QE-R).

Pseudo free-standing method

The films were spin-coated on top of the PEDOT:PSS layer on glass and a nanosecond laser patterning technique was used to carve out dog-bone film specimens. Then film specimens were transferred to the water surface and attached to PDMS clamps. The tensile test was performed by applying a tensile strain using a linear displacement stage at a speed of 0.5 mm/min.

GIWAXS and GISAXS

GIWAXS data were obtained at beamline BL16B1 of Shanghai Synchrotron Radiation Facility (SSRF). The monochromatic of the light source was 1.24 Å. The data were recorded by using the two-dimensional image plate detector of Pilatus 1M from Dectris, Switzerland.

GISAXS data of films were obtained at beamline BL16B1 of Shanghai Synchrotron Radiation Facility (SSRF). The monochromatic of the light source was 1.24 Å. The incidence angle was 0.2°, and the sample-to-detector distance was 2200 mm by calibration for GISAXS.

GISAXS Model Fitting

The GISAXS 1D profiles were fitted with a universal model following Equation (1). Data fitting was done using SasView (version 5.01) software.

$$I(q) = \frac{A_1}{[1 + (q\xi)^2]^2} + A_2 \langle P(q,R) \rangle \; S(q, R, \eta, D) + B \tag{1}$$

$$S(q) = 1 + \frac{sin[(D-1)tan^{-1}(q\eta)]b \pm \sqrt{b^2 - 4ac}}{(qR)^D} \frac{D\Gamma(D-1)}{[1 + \frac{1}{(q\eta)^2}]^{(D-1)/2}} \tag{2}$$

where A_1, A_2, and B are independent fitting parameters and q is the scattering wave vector. The average correlation length ξ of the PM6 domain and the Debye-Andersone-Brumberger (DAB) term make up the first term. The contribution from BTP-eC9 fractal-like aggregations is seen by the second term. Here, R is the mean spherical radius of the primary BTP-eC9 particles, P

(q, R) is the form factor of the BTP-eC9, S (q, R, η, D) is the fractal structure factor to explain the primary particles interaction in this fractal-like aggregation system, η is the correlation length of the fractal-like structure, and D is the fractal dimension of the network. Equation 3 was used to calculate the average domain size by the Guinier radius of the fractallike network R_g.

$$R_g = \eta \sqrt{\frac{D(D+1)}{2}} \tag{3}$$

TPV and TPC

The transient photovoltage (TPV) measurement was conducted under 1 sun illumination with a white light-emitting diode, and the device was set to the open-circuit condition. While the device was set to the short-circuit condition in the dark for the transient photocurrent (TPC) measurement. The output signal was collected by keysight oscilloscope for both TPV and TPC.

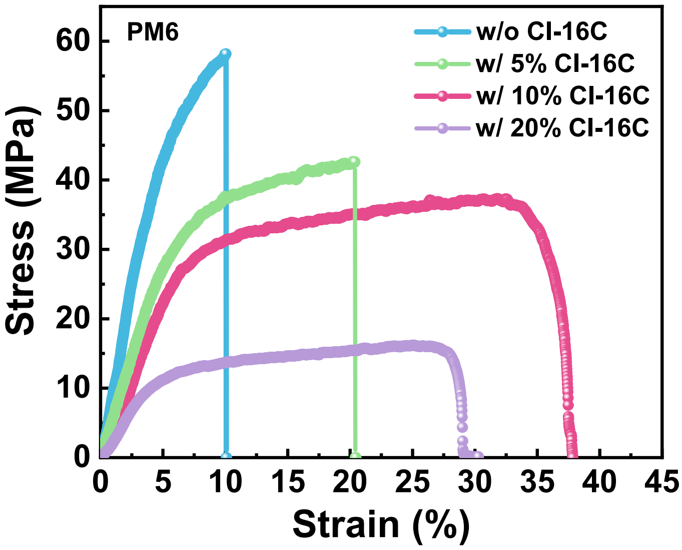

Fig. S1 The stress-strain curves of PM6 films with different concentrations processed with and without Cl-16C using the pseudo free-standing method.

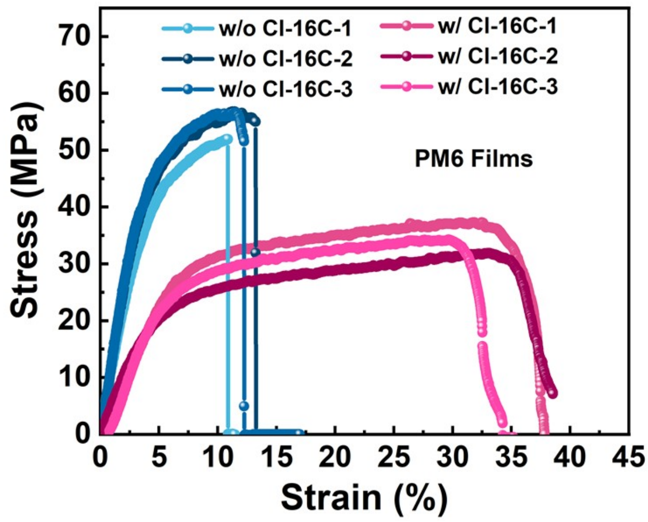

Fig. S2 Stress-train curves of PM6 films processed with and without Cl-16C obtained from three experiments.

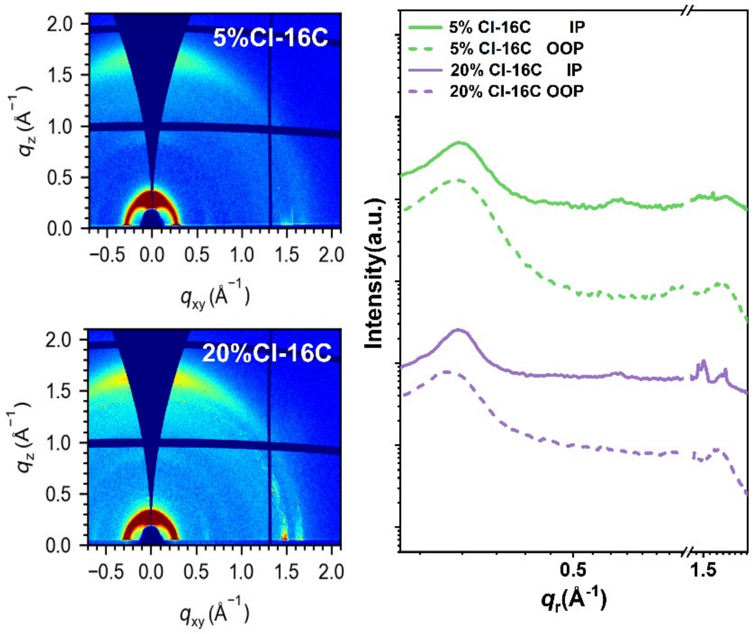

Fig. S3 2D GIWAXS patterns and the corresponding 1D line-cut profiles of the PM6 films processed with 5 vol% and 20 vol% Cl-16C.

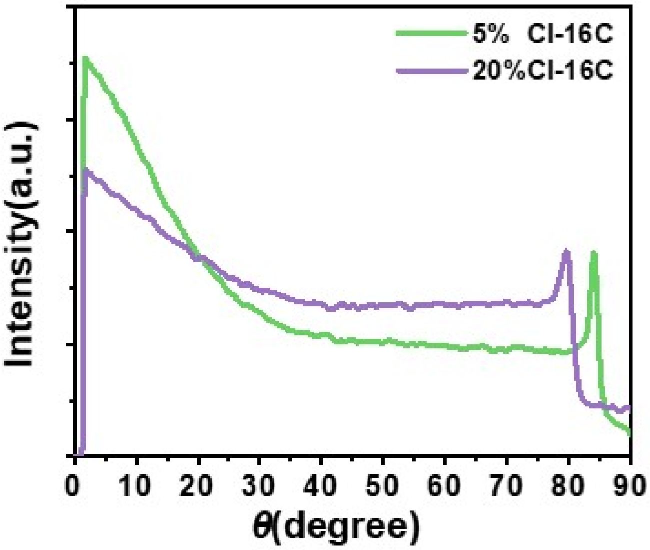

Fig. S4 Pole figure of the lamellar peak of the PM6 films processed with 5 vol% and 20 vol% Cl-16C.

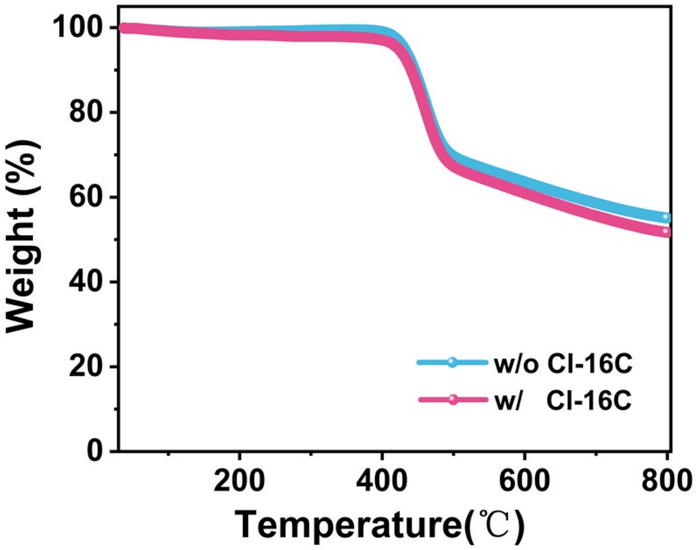

Fig. S5 TGA curves of PM6 films processed with and without Cl-16C.

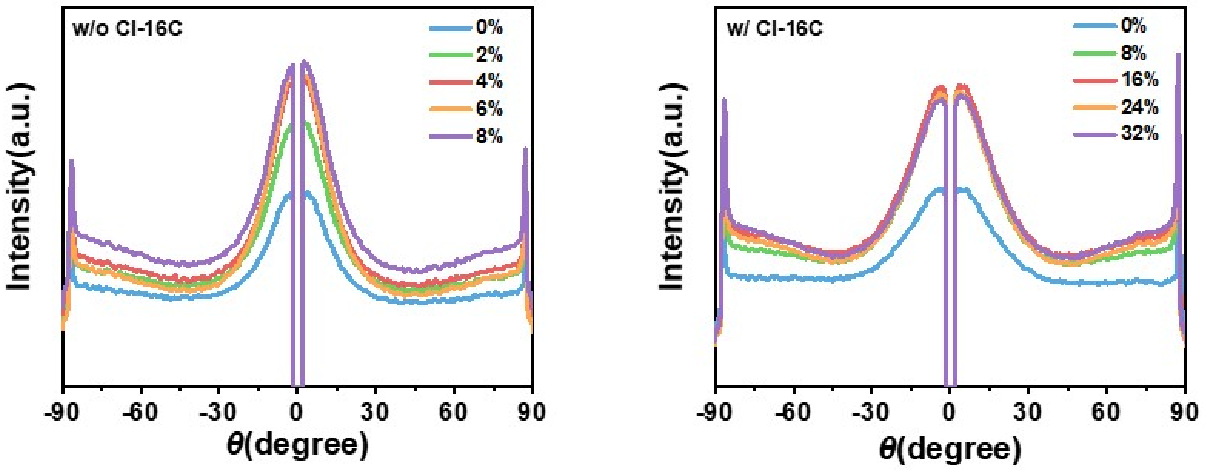

Fig. S6 Pole figure of the lamellar peak of the PM6 films processed with and without 10 vol% Cl-16C under various strains.

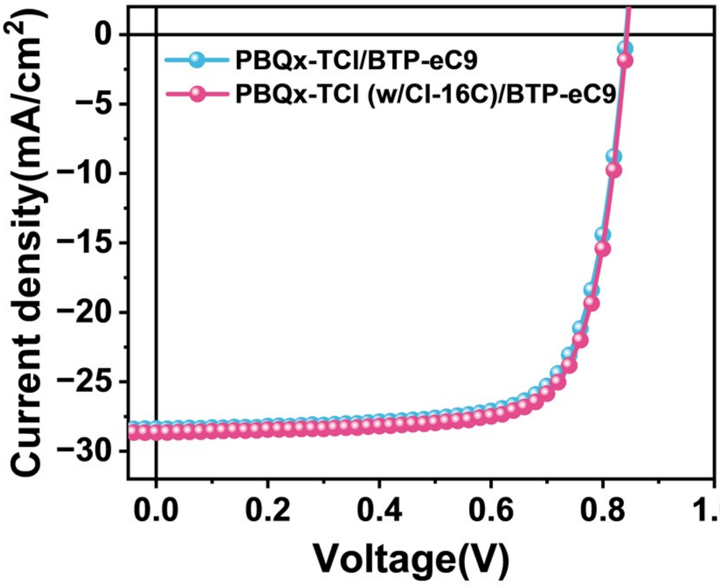

Fig. S7 J-V curves of OPV devices based on PBQx-TCl/BTP-eC9 and PBQx-TCl (w/Cl-16C)/BTP-eC9

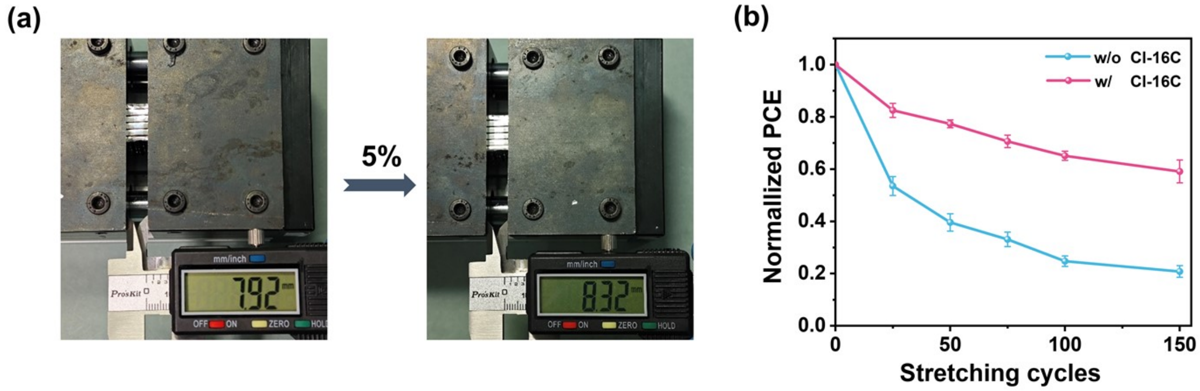

Fig. S8 (a) Images of cyclic stretching tests of flexible OPVs. (b) PCE retention during 150 stretching cycles (ε = 5%) for devices processed with/without Cl-16C.

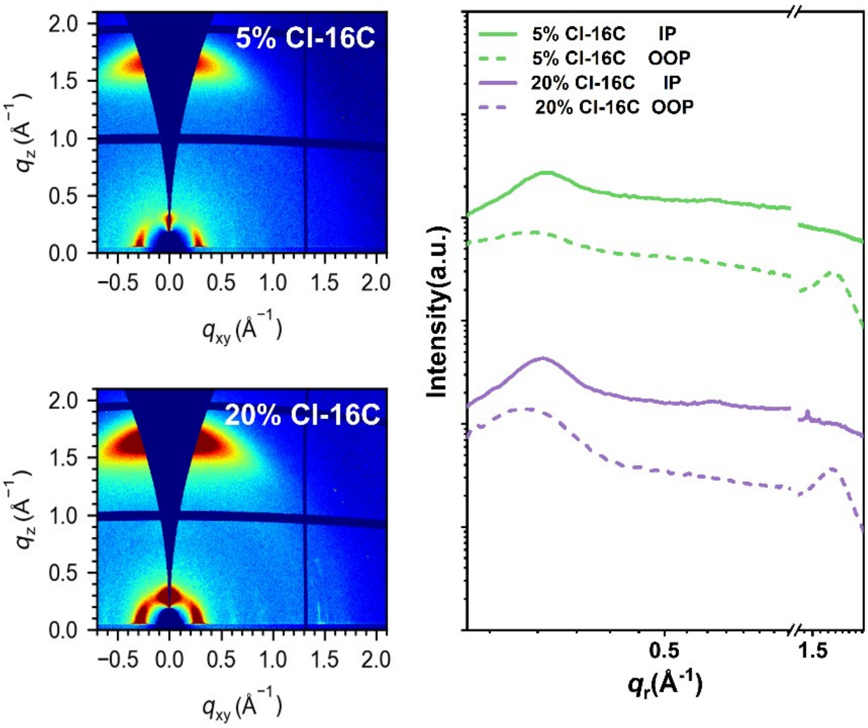

Fig. S9 2D GIWAXS patterns and the corresponding 1D line-cut profiles of the PM6/BTP-eC9 films processed with 5 vol% and 20 vol% Cl-16C.

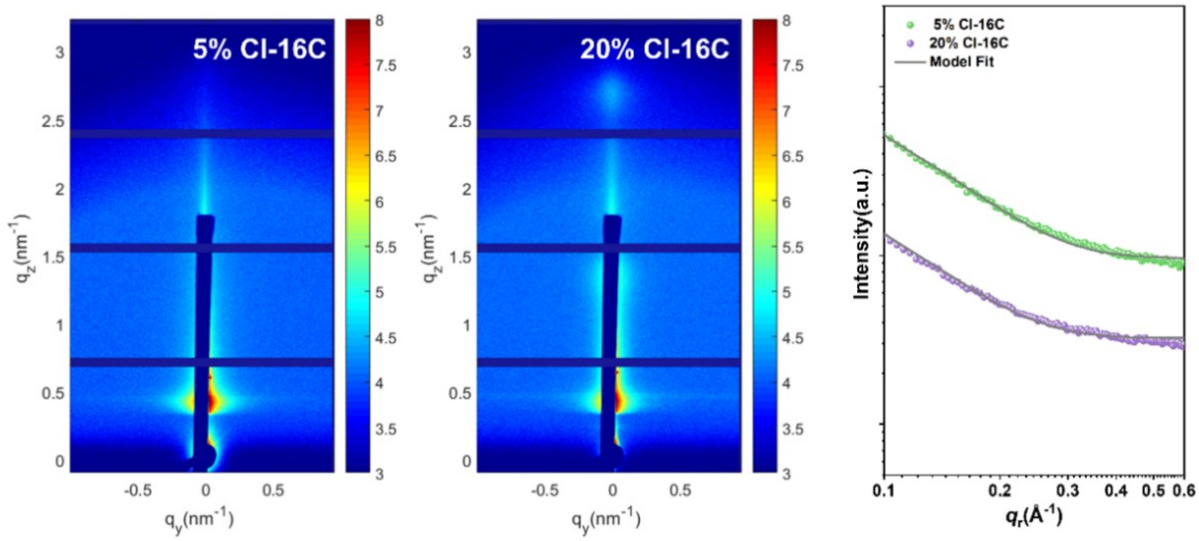

Fig. S10 2D GISAXS patterns and the corresponding 1D line profiles of the PM6/BTP-eC9 films processed with 5 vol% and 20 vol% Cl-16C.

Table S1 The values of *q* and *d*-spacing extracted from the lamellar and π-π peaks at the OOP direction of the PM6 films processed without and with Cl-16C.

condition	*q* (Å^{-1})		*d*-spacing (Å)	
	Lamellar packing	π-π packing	Lamellar packing	π-π packing
w/o Cl-16C	0.283	1.62	22.2	3.88
5% Cl-16C	0.275	1.64	22.8	3.83
10% Cl-16C	0.260	1.64	24.2	3.83
20% Cl-16C	0.258	1.62	24.4	3.88

Table S2 The values of *q* and *d*-spacing extracted from the lamellar and π-π peaks at the IP direction of the PM6 films proocessed without and with Cl-16C.

condition	*q* (Å^{-1})		*d*-spacing (Å)	
	Lamellar packing	π-π packing	Lamellar packing	π-π packing
w/o Cl-16C	0.283	\	22.2	\
5% Cl-16C	0.273	\	23.0	\
10% Cl-16C	0.275	1.68	22.8	3.74
20% Cl-16C	0.273	1.69	23.0	3.72

Table S3 The contents of the face-on and edge-on regions using the intensity distribution of the lamellar peak as a function of the azimuth angle (*θ*) of the PM6 films processed without and with Cl-16C.

condition	Face-on Fraction	Edge-on Fraction
w/o Cl-16C	46%	54%
5% Cl-16C	34%	66%
10% Cl-16C	38%	62%
20% Cl-16C	41%	59%

Table S4 Molecule packing parameters extracted from the lamellar peak at the OOP direction of the PM6 films without Cl-16C under various strains at α=0°.

Strain (%)	q (Å^{-1})	d-spacing (Å)	$FWHM$ (Å^{-1})	CCL (Å)
0	0.29	21.7	0.088	63.5
2	0.29	21.8	0.089	62.8
4	0.29	21.7	0.090	62.1
6	0.29	21.7	0.092	60.8
8	0.29	21.7	0.098	57.1

Table S5 Molecule packing parameters extracted from the lamellar peak at the IP direction of the PM6 films without Cl-16C under various strains at α=0°.

Strain (%)	q (Å^{-1})	d-spacing (Å)	$FWHM$ (Å^{-1})	CCL (Å)
0	0.298	21.1	0.095	58.9
2	0.3	20.9	0.103	54.3
4	0.3	20.9	0.103	54.3
6	0.293	21.4	0.101	55.4
8	0.3	20.9	0.103	54.3

Table S6 Molecule packing parameters extracted from the lamellar peak at the OOP direction of the PM6 films without Cl-16C under various strains at *α*=90°.

Strain (%)	*q* (Å^{-1})	*d*-spacing (Å)	*FWHM* (Å^{-1})	*CCL* (Å)
0	0.285	22.0	0.089	62.8
2	0.285	22.0	0.083	67.4
4	0.29	21.7	0.096	58.3
6	0.29	21.7	0.089	62.8
8	0.29	21.7	0.093	60.1

Table S7 Molecule packing parameters extracted from the lamellar peak at the IP direction of the PM6 films without Cl-16C under various strains at *α*=90°.

Strain (%)	*q* (Å^{-1})	*d*-spacing (Å)	*FWHM* (Å^{-1})	*CCL* (Å)
0	0.295	21.3	0.093	60.1
2	0.29	21.7	0.101	55.4
4	0.3	20.9	0.117	47.8
6	0.288	21.8	0.101	55.4
8	0.288	21.8	0.114	49.1

Table S8 Molecule packing parameters extracted from the lamellar peak at the OOP direction of the PM6 films with Cl-16C under various strains at α=0°.

Strain (%)	q (Å^{-1})	d-spacing (Å)	$FWHM$ (Å^{-1})	CCL (Å)
0	0.29	21.7	0.073	76.6
8	0.288	21.8	0.071	78.8
16	0.285	22.0	0.071	78.8
24	0.285	22.0	0.071	78.8
32	0.288	21.8	0.072	77.7

Table S9 Molecule packing parameters extracted from the lamellar peak at the IP direction of the PM6 films with Cl-16C under various strains at α=0°.

Strain (%)	q (Å^{-1})	d-spacing (Å)	$FWHM$ (Å^{-1})	CCL (Å)
0	0.293	21.4	0.055	101.7
8	0.295	21.3	0.053	105.5
16	0.298	21.1	0.054	103.6
24	0.298	21.1	0.054	103.6
32	0.298	21.1	0.054	103.6

Table S10 Molecule packing parameters extracted from the lamellar peak at the OOP direction of the PM6 films with Cl-16C under various strains at α=90°.

Strain (%)	q (Å^{-1})	d-spacing (Å)	$FWHM$ (Å^{-1})	CCL (Å)
0	0.29	21.7	0.071	78.8
8	0.288	21.8	0.069	81.0
16	0.285	22.0	0.069	81.0
24	0.285	22.0	0.067	83.5
32	0.285	22.0	0.069	81.0

Table S11 Molecule packing parameters extracted from the lamellar peak at the IP direction of the PM6 films with Cl-16C under various strains at α=90°.

Strain (%)	q (Å^{-1})	d-spacing (Å)	$FWHM$ (Å^{-1})	CCL (Å)
0	0.293	21.4	0.053	105.5
8	0.29	21.7	0.059	94.8
16	0.29	21.7	0.062	90.2
24	0.29	21.7	0.058	96.4
32	0.29	21.7	0.068	82.2

Table S12 The values of integrated area of the curves of the lamellar peak of the PM6 films processed with and without Cl-16C under various strains.

w/o Cl-16C		w/ Cl-16C	
Strain (%)	integrated area of the curves	Strain (%)	integrated area of the curves
0	1.1×10^{7}	0	1.6×10^{7}
2	1.3×10^{7}	8	2.0×10^{7}
4	1.5×10^{7}	16	2.2×10^{7}
6	1.4×10^{7}	24	2.1×10^{7}
8	1.6×10^{7}	32	2.2×10^{7}

Table S13 Molecule packing parameters extracted from the lamellar peak at the IP direction of the PM6/BTP-eC9 films without and with different concentrations of Cl-16C.

Concentration	q (Å^{-1})	d-spacing (Å)	$FWHM$ (Å^{-1})	CCL (Å)
0	0.293	21.4	0.086	65.0
5%	0.283	22.2	0.085	65.8
10%	0.288	21.8	0.084	66.6
20%	0.285	22.0	0.078	71.7

Table S14 Molecule packing parameters extracted from the π-π peak at the OOP direction of the PM6/BTP-eC9 films without and with different concentrations of Cl-16C.

Concentration	q (Å^{-1})	d-spacing (Å)	$FWHM$ (Å^{-1})	CCL (Å)
0	1.68	3.74	0.218	25.7
5%	1.66	3.79	0.215	26.0
10%	1.64	3.83	0.207	27.0
20%	1.64	3.83	0.202	27.7

Table S15 The fitting parameters of GISAXS measurement of PM6/BTP-eC9 films without and with different concentration of Cl-16C.

Concentration	ξ (nm)	η(nm)	D	$2R_g$(nm)
0	22.6	6.5	2.3	25.3
5%	23.4	6.8	2.5	28.4
10%	25.5	7.1	2.5	29.7
20%	24.8	7.0	2.4	28.3

Table S16. Photovoltaic parameters of OPVs with and without Cl-16C.

Active layer	V_{OC} (V) [a]	J_{SC} (mA cm^{-2}) [a]	FF (%) [a]	PCE (%) [a]
PBQx-TCl/BTP-eC9	0.840 (0.837±0.007)	28.4 (28.4±0.4)	74.0 (73.8±0.5)	17.7 (17.6±0.1)
PBQx-TCl (w/Cl-16C)/ BTP-eC9	0.842 (0.839±0.003)	28.7 (28.5±0.1)	74.8 (74.7±0.5)	18.1 (17.9±0.2)

[a] Average value of eight independent devices in parentheses.